

- (15) Bilbo, A. J.; Sharts, C. M. *J. Polym. Sci., Part A-1* **1967**, *5*, 2891.
- (16) Horn, H.-G. *Makromol. Chem.* **1970**, *138*, 163.
- (17) Horn, H.-G.; Steger, W. *Makromol. Chem.* **1974**, *175*, 1777.
- (18) Washburn, R. M.; Baldwin, R. A. U.S. Patents 3341477 and 3341478, 1967; *Chem. Abstr.* **1967**, *67*, 100585w, 100586x.
- (19) Wiegräbe, W.; Bock, H. *Chem. Ber.* **1968**, *101*, 1414. Thomas, L. C. *Interpretation of the Infrared Spectra of Organophosphorus Compounds*; Heyden: London, 1974; Chapter 10.
- (20) Lambert, J. B.; Shurvell, H. F.; Lightner, D. A.; Cooks, G. R. *Introduction to Organic Spectroscopy*; Macmillan: New York, 1987; Chapter 7.
- (21) Mark, V.; Dungan, C. H.; Crutchfield, M. M.; Van Wazer, J. R. In  $^{31}\text{P}$  Nuclear Magnetic Resonance. *Topics in Phosphorus Chemistry*; Crutchfield, M. M., Dungan, C. H., Letcher, J. H., Mark, V., Van Wazer, J. R., Eds.; Interscience: New York, 1967; Vol. 5, Chapter 4.
- (22) Fyfe, C. A. *Solid State NMR for Chemists*; CFC Press: Guelph, ON, Canada, 1983; Chapter 6. Komoroski, R. A. In *High Resolution NMR Spectroscopy of Synthetic Polymers in Bulk*; Komoroski, R. A., Ed.; VCH Publishers: Deerfield Beach, FL, 1986; Chapter 2.
- (23) Wendlandt, W. W. *Thermal Analysis*, 3rd ed.; Wiley: New York, 1986; p 10.
- (24) Shalaby, S. W. In *Thermal Characterization of Polymeric Materials*; Turi, E. A., Ed.; Academic: New York, 1981; Chapter 3.
- (25) Kricheldorf, H. R.; Müller, D. *Macromolecules* **1983**, *16*, 615.
- (26) Earl, W. L.; Vanderhart, D. L. *J. Magn. Reson.* **1982**, *48*, 35.
- (27) Baldwin, R. A.; Cheng, M. T. *J. Org. Chem.* **1967**, *32*, 1572.

## Synthesis and Solution Properties of Extended Chain Poly(2,6-benzothiazole) and Poly(2,5-benzoxazole)

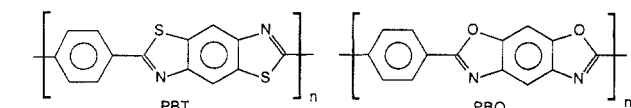
Andrea W. Chow,\* Steven P. Bitler, Paul E. Penwell, Dyan J. Osborne, and James F. Wolfe\*<sup>†</sup>

Chemistry Laboratory, SRI International, 333 Ravenswood Avenue, Menlo Park, California 94025. Received October 25, 1988; Revised Manuscript Received February 27, 1989

**ABSTRACT:** The  $\text{P}_2\text{O}_5$  adjustment method allows polymerization of poly(2,6-benzothiazole) (ABPBT) and poly(2,5-benzoxazole) (ABPBO) in poly(phosphoric acid) at high concentrations up to 21 wt %. ABPBO can also be prepared in methanesulfonic acid by adding up to 45 wt %  $\text{P}_2\text{O}_5$ . When polymerized at concentrations above ~14 wt %, the reacting mixture became liquid crystalline and the molecular weight of the resulting polymer was significantly higher than that of mixtures polymerized in the isotropic phase (below ~14 wt %). Addition of monofunctional end-capping agents to the starting mixture depressed the final molecular weight of the polymeric products, and Flory's theory for condensation polymerization appeared to predict the degree of molecular weight depression. Dilute solution characterization of these poly(benzazole) polymers indicated stiff-chain conformations, and comparison with the Yamakawa-Fujii wormlike chain model suggested that they have persistence lengths of 90–130 Å. The Mark-Houwink-Sakurada constants for these semirigid polymers were also determined.

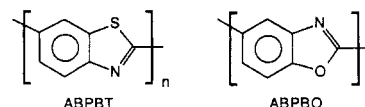
### Introduction

Our studies of aromatic heterocyclic polymers of the poly(benzazole) family are motivated by the need for lightweight, high-strength, high-modulus, environmentally resistant materials for use in structural applications. Within the Air Force's Ordered Polymers Research Program, our original approach focused on the rigid-rod polymer structures poly(*p*-phenylenebenzo[1,2-*d*:4,5-*d'*]-bisthiazole) (PBT)<sup>1</sup> and poly(*p*-phenylenebenzo[1,2-*d*:5,4-*d'*]bisoxazole) (PBO),<sup>2</sup> which formed liquid-crystalline phases during polymerization at concentrations above 5 wt %.<sup>3</sup> The catenation angle, which is the angle between exocyclic bonds of the rigid backbone units, is 180° for both PBT and PBO. These structures thereby provide some of the most rodlike configurations in the poly(benzazole) family.



While developing the synthesis methods for preparing PBT in poly(phosphoric acid) (PPA), we discovered that polymerization proceeded at polymer concentrations as

high as 21 wt % if the  $\text{P}_2\text{O}_5$  content of PPA was increased to account for the greater relative amount of water of condensation.<sup>4</sup> The ability to polymerize at such high concentrations led to the discovery that polymers with catenation angles much less than 180°, such as poly(2,6-benzothiazole) (ABPBT) and poly(2,5-benzoxazole) (ABPBO), also formed the liquid-crystalline phase during polymerization.



ABPBT and ABPBO are characterized by catenation angles of 162° and 150°, respectively. Because of the unrestricted rotation between repeat units,<sup>5</sup> these backbone diads can assume either an extended chain conformation (trans) or a coil-like conformation (cis), as illustrated in Figure 1. In dilute solution, these polymers are likely to assume a random distribution of cis and trans conformations if neither conformation is statistically favored. At high concentrations, the liquid-crystalline phase is favored energetically, and the trans conformation is believed to dominate to allow this phase change.

We report the synthesis method for polymerizing these poly(benzazoles) with controlled molecular weights and the determination of their dilute solution properties by low-angle light-scattering and viscometry measurements. We

\* To whom correspondence should be addressed.

<sup>†</sup> Current address: Lockheed Missiles & Space Co., 3251 Hanover St., Palo Alto, CA 94304.

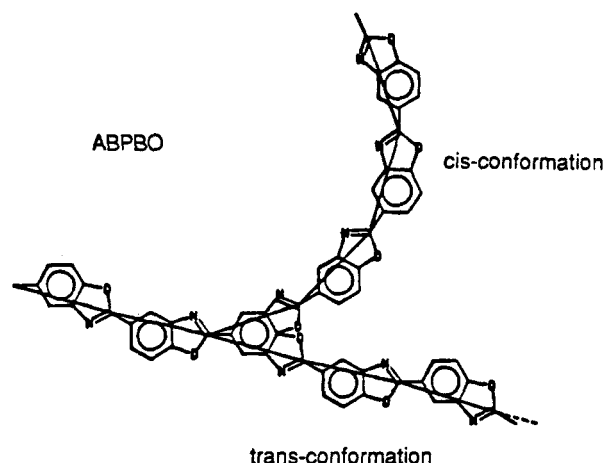
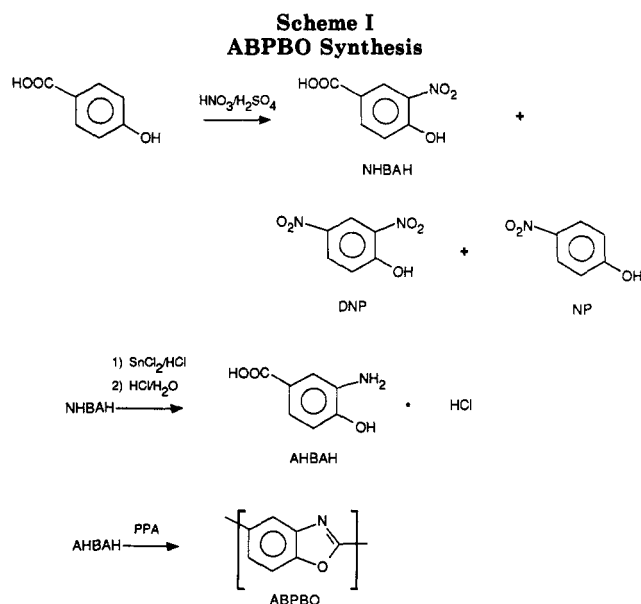


Figure 1. Schematic illustration of the coil-like and extended chain conformations of ABPBO.



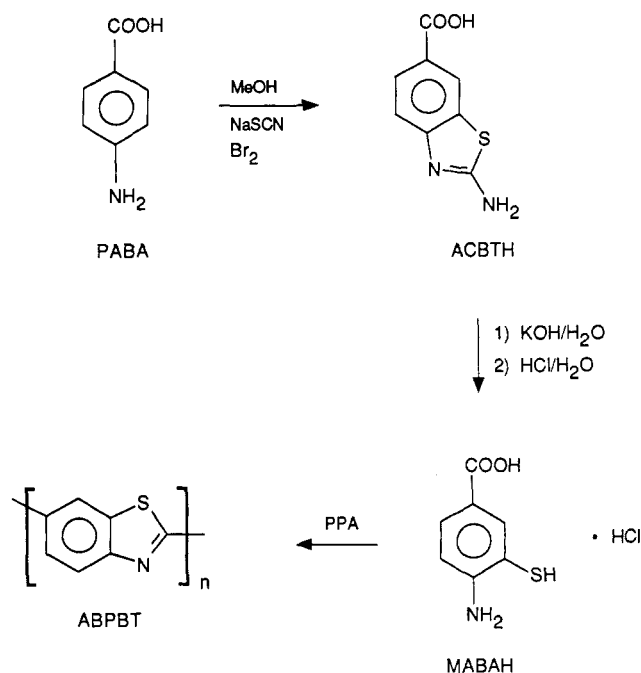
also compare the experimental data with a wormlike chain model.

### Experimental Section

**ABPBO Monomer Synthesis.** 3-Amino-4-hydroxybenzoic acid hydrochloride (AHBAH) was prepared in two steps from *p*-hydroxybenzoic acid,<sup>6</sup> by nitration with 1 equiv of nitric acid in glacial acetic acid at low temperature followed by reduction with stannous chloride and hydrochloric acid, as illustrated in Scheme I. Typical yields for the two steps were 40% and 90–95%, respectively. AHBAH was heated in water containing 1 wt % stannous chloride and obtained as small, colorless needles by adding an equal volume of concentrated hydrochloric acid. After washing with concentrated hydrochloric acid and diethyl ether, AHBAH was obtained without water of hydration by drying for 16 h at about 65 °C under reduced pressure. Anal. Calcd for  $C_7H_6NO_3Cl$ : C, 44.34; H, 4.25; N, 7.39; Cl, 18.70. Found: C, 44.41; H, 4.32; N, 7.33; Cl, 18.87.

**ABPBT Monomer Synthesis.** 3-Mercapto-4-aminobenzoic acid hydrochloride (MABAH) was prepared in two steps from *p*-aminobenzoic acid (PABA), as illustrated in Scheme II, by dissolving PABA (6.0 mol) and sodium thiocyanate (12.7 mol) in 6 L of methanol and adding bromine (6.35 mol) over a 3.5-h period, while maintaining the pot temperature at –5 to –10 °C. After stirring for an additional 2 h at about 5 °C, the resulting yellow precipitate was collected by filtration, washed with water, and recrystallized twice from 6 L of 1 N hydrochloric acid by heating to about 70 °C, filtering, and then adding 3 L of concentrated hydrochloric acid to the filtrate. Upon cooling, the 2-amino-6-carboxybenzothiazole hydrochloride (ACBTH) was obtained as

**Scheme II**  
**ABPBT Synthesis**



colorless needles in 50% yield: mp 288–290 °C (dec). ACBTH was hydrolyzed by heating 100 g in 800 g of 50% aqueous potassium hydroxide at the reflux temperature for 4 h. The reaction mixture was filtered, and the filtrate was added to 575 mL of cold, concentrated hydrochloric acid. The precipitate was collected and recrystallized twice from 1.5 L of water by adding hydrochloric acid until the product dissolved, adding 5 g of stannous chloride, heating to 70 °C, adding an additional liter of concentrated hydrochloric acid, and cooling. The yield was 29 g (33%) of MABAH: mp 192–194 °C; IR 3380 (O–H), 3000 (N–H), 2520 (S–H), 1700 (C=O), 1605  $cm^{-1}$  (C=C). Anal. Calcd for  $C_7H_6NO_3S$ : C, 40.88; H, 3.92; N, 6.81; S, 15.59; Cl, 17.24. Found: C, 40.67; H, 3.91; N, 6.85; S, 15.78; Cl, 17.10.

**Polymer Synthesis.** The general method for preparing benzazole polymers in PPA in the nematic phase at polymer concentrations greater than 10 wt % has been reviewed.<sup>7</sup> The key polymerization variables employed in this technique, which we call the  $P_2O_5$  adjustment method, relate to the proper control of PPA composition at various stages of polymerization based on the concentration of the condensing species.

The variables relating to the  $P_2O_5$  adjustment of PPA are (1) initial  $P_2O_5$  content of the PPA,  $P_1$ , which is operative during the initial step of hydrogen chloride removal or dehydrochlorination; (2) intermediate  $P_2O_5$  content of the PPA,  $P_2$ , obtained by adding  $B$  grams of powdered  $P_2O_5$  to the initial PPA/monomer mixture after hydrogen chloride removal; (3) final  $P_2O_5$  content of the PPA,  $P_3$ , achieved by hydrolysis of the intermediate PPA, having a  $P_2O_5$  content of  $P_2$ , by the water of polycondensation; (4) polymer concentration,  $C$ , the weight fraction of polymer in the total weight of the solution; (5) polymer yield,  $Y$ ; (6) weight of initial PPA used for the dehydrochlorination,  $A$ , given by

$$A = \frac{Y[1 - P_3][(1/C) - 1] - 36.03/M}{1 - P_1}$$

where  $M$  is the weight of the polymer that produces 2 mol of water of condensation; (7) weight of  $P_2O_5$  required to achieve a chosen  $P_3$ ,  $B$ , given by

$$B = Y[(1/C) - 1 - 36.03/M] - A$$

(8) amount of monofunctional reagent, or end capper, EC%, given in moles per 100 mol of monomer; (9) polymerization time, PT, defined as the time that the polymerization mixture was heated above 100 °C.

Typical ABPBT and ABPBO polymerizations are outlined in Tables I and II by giving these nine variables and the intrinsic viscosities of the resulting polymers.

**Table I**  
**Polymerizations of MABAH with EC% of Monofunctional Reagent (*M* = 133.17)**

ABPBT <sup>a</sup>	<i>P</i> <sub>1</sub> , %	<i>P</i> <sub>2</sub> , %	<i>P</i> <sub>3</sub> , %	<i>C</i> , %	<i>Y</i> , g	<i>A</i> , g	<i>B</i> , g	EC%	PT, <sup>b</sup> h	[ $\eta$ ], dL/g
-1	77.3	89.5	83.4	20.1	30.0	51.65	59.72	0	48	11.5
-2	77.3	87.5	82.3	17.9	26.55	63.32	51.34	0	36	8.14
-3	77.2	86.5	82.7	13.9	10.0	35.00	24.06	0	24 <sup>f</sup>	7.55
-4	77.0	87.9	83.0	17.0	10.0	24.3	22.0	0.5 <sup>d</sup>	21	4.18
-5	77.0	87.9	83.0	17.0	10.0	24.3	22.0	1.0 <sup>d</sup>	21	2.11
-6 <sup>c</sup>	77.0	87.9	83.0	17.0	10.0	24.3	22.0	5.0 <sup>e</sup>	21	0.76
-7 <sup>c</sup>	77.0	87.9	83.0	17.0	10.0	24.3	22.0	10.0 <sup>e</sup>	21	0.27

<sup>a</sup> All polymerization mixtures, which are characterized by PPA having a P<sub>2</sub>O<sub>5</sub> content between *P*<sub>2</sub> and *P*<sub>3</sub> (depending on the extent of reaction) and polymer concentration and intrinsic viscosity as indicated, were liquid crystalline except those indicated by footnote *c* (isotropic). <sup>b</sup> After removal of hydrogen chloride and addition of *B* grams of P<sub>2</sub>O<sub>5</sub> at temperatures below 100 °C, all PPA/monomer mixtures were heated within 1 h to 185 °C and maintained at that temperature unless otherwise noted. <sup>c</sup> Isotropic. <sup>d</sup> Benzoic acid was the monofunctional reagent. <sup>e</sup> Nicotinic acid as the monofunctional reagent. <sup>f</sup> Heated at 175 °C for the time indicated in column PT.

**Table II**  
**Polymerizations of AHBAH with EC% of Benzoic Acid (*M* = 117.11)**

ABPBO <sup>a</sup>	<i>P</i> <sub>1</sub> , %	<i>P</i> <sub>2</sub> , %	<i>P</i> <sub>3</sub> , %	<i>C</i> , %	<i>Y</i> , g	<i>A</i> , g	<i>B</i> , g	EC% <sup>b</sup>	PT, <sup>c</sup> h	[ $\eta$ ], dL/g
-1	77.3	87.85	82.2	17.3	10.2	24.4	21.28	0	28	15.0
-2a <sup>d</sup>	77.2	88.4	83.0	16.5	10.0	26.65	25.55	0	1.5	1.1
-2b <sup>d</sup>									2.3	2.8
-2c <sup>d</sup>									5.6	7.1
-2d <sup>d</sup>									7.5	8.6
-2e <sup>d</sup>									24.5	17.4
-2f <sup>d</sup>									29.8	18.0
-3a <sup>d</sup>	77.2	88.4	83.0	16.5	8.0	19.37	18.74	0	4.0 <sup>f</sup>	13.7
-3b <sup>d</sup>									5.1 <sup>f</sup>	17.6
-3c <sup>d</sup>									7.3 <sup>f</sup>	17.6
-3d <sup>d</sup>									23.3 <sup>f</sup>	24.1
-3e <sup>d</sup>									26.7 <sup>f</sup>	21.5
-3f <sup>d</sup>									29.7 <sup>f</sup>	16.4
-4	77.6	87.5	82.2	16.7	17.8	28.65	22.82	0	40	13.8
-5 <sup>e</sup>	77.2	86.6	83.0	13.6	10.0	41.24	29.23	0	29.5	9.2
-6a	77.3	87.4	83.02	13.9	10.0	32.59	25.96	0	6.5 <sup>g</sup>	3.85
-6b									24.0 <sup>g</sup>	12.7
-7	73.9	89.7	83.6	17.0	10.0	17.56	27.1	0.5	20.0	4.95
-8	73.9	89.7	83.6	17.0	10.0	17.56	27.2	1.0	18.0	3.39
-9 <sup>e</sup>	78.0	91.0	85.0	16.0	11.49	22.45	31.1	5.0	25.0	0.62

<sup>a</sup> All polymerization mixtures, which are characterized by PPA having a P<sub>2</sub>O<sub>5</sub> content between *P*<sub>2</sub> and *P*<sub>3</sub> (depending on the extent of reaction) and polymer concentration and intrinsic viscosity as indicated, were liquid crystalline except those indicated by footnote *e* (isotropic). <sup>b</sup> Benzoic acid was the monofunctional reagent. <sup>c</sup> After removal of hydrogen chloride and addition of *B* grams of P<sub>2</sub>O<sub>5</sub> at temperatures below 100 °C, all PPA/monomer mixtures were heated within 1 h to 185 °C and maintained at that temperature unless otherwise noted. <sup>d</sup> The same monomer sample was used for these polymerizations. <sup>e</sup> Isotropic. <sup>f</sup> ABPBO-3a-f were heated at 200 °C for the time indicated in column PT. <sup>g</sup> ABPBO-6a and -6b were heated at 175 °C for the time indicated in column PT. Both samples were optically isotropic at 175 °C but were birefringent at room temperature.

In another experiment, ABPBO was prepared in methanesulfonic acid (MSA) instead of PPA using the P<sub>2</sub>O<sub>5</sub> adjustment method to demonstrate the general utility of the method. The results of this experiment are discussed in the following section.

After polymerization, all polymer samples were precipitated in water, washed with water in a Soxhlet extractor to remove residual PPA, and dried under reduced pressure at 130–140 °C for 24 h to ensure complete removal of moisture. The dried samples were stored in a desiccator until use. MSA was used as solvent for dilute solution measurements, and it was distilled under reduced pressure and stored under dry nitrogen. The polymer solutions were analyzed within 3 days of preparation.

**Light Scattering from Semirigid Polymers.** Light-scattering measurements were made by using a Chromatix KMX-6 (LDCO Milton Roy) low-angle light-scattering (LALS) photometer equipped with a polarizing filter to allow measurements of the vertical and horizontal components of the scattered light. The incident wavelength is 632.8 nm. Annulus of 6–7° and field stop of 0.2 mm were used. A narrow band interference filter was inserted between the sample and the detector to remove fluorescence radiation from the sample. All solvents and polymer solutions for light scattering were filtered through 0.2- $\mu$ m (Millipore) membrane filters. The differential refractive index increments,  $dn/dc$ , were measured for each polymer sample in MSA using a 632.8-nm laser. Values for  $dn/dc$  range from 0.42 to 0.54 dL/g for ABPBT and from 0.31 to 0.43 dL/g for ABPBO. All measurements were performed at ambient temperatures of 23  $\pm$  2 °C.

Light scattering from an anisotropic element of a polymer chain involves the intrinsic anisotropy factor  $\delta_0$  defined as<sup>8</sup>

$$\delta_0^2 = \frac{(\alpha_1 - \alpha_2)^2 + (\alpha_1 - \alpha_3)^2 + (\alpha_2 - \alpha_3)^2}{2(\alpha_1 + \alpha_2 + \alpha_3)^2} \quad (1)$$

where  $\alpha_1$ ,  $\alpha_2$ , and  $\alpha_3$  are the principal polarizabilities of the scattering element. The overall anisotropy of the chain,  $\delta$ , is dependent on the chain conformation in addition to  $\delta_0$ .  $\delta$  can be defined as an average of  $\delta_0$  for each chain segment over the conformation space. For a wormlike chain with contour length *L* and persistence length  $\rho$ ,  $\delta$  derived from theory<sup>9</sup> is

$$\delta^2 = \delta_0^2 \left( \frac{2}{3Z} \right) \{1 - \exp(-3Z)\} \quad (2)$$

where  $Z = L/\rho$ .

For LALS, the equations describing the Rayleigh ratios  $R_{Vv}$  and  $R_{Hv}$  for the vertical and horizontal components of light scattered in the transverse plane with vertically polarized incident light can be written as<sup>10</sup>

$$\lim_{c \rightarrow 0} [R_{Vv}/KMc] = 1 + \frac{4}{5}\delta^2 - 2A_2Mc + O(c^2) \quad (3)$$

$$\lim_{c \rightarrow 0} [R_{Hv}/KMc] = \frac{3}{5}\delta^2 + O(c^2) \quad (4)$$

$A_2$  is the second virial coefficient, *M* is the molecular weight, and *c* is the solution concentration. *K* is an optical constant equal

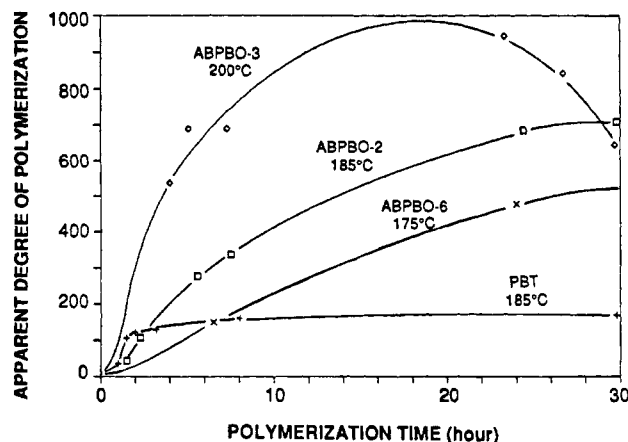


**Figure 2.** Plot of the apparent degree of polymerization as a function of reaction time for ABPBO polycondensation at various reaction temperatures. The polymerization progress of PBT is included for comparison.

to  $4\pi^2 n^2 (dn/dc)^2 / \lambda^4 N_A$ , where  $n$  is the refractive index of the solvent,  $\lambda$  is the wavelength of the laser light, and  $N_A$  is Avogadro's number. For a polydisperse polymer,  $M$  obtained from light-scattering measurements is the weight-average molecular weight ( $M_w$ ).

**Intrinsic Viscosity.** Intrinsic viscosity measurements were determined in MSA at  $30.0 \pm 0.2$  °C using a Ubbelohde viscometer. For all dilutions, the flow times were above 110 s and the kinetic energy correction was considered negligible. Solution concentrations were chosen such that the flow time ratio of solution to solvent is between 1.1 and 1.5. The Huggins and Kraemer equations were used to calculate  $[\eta]$ :

$$\eta_{sp}/c = [\eta] + k'[\eta]^2 c \quad (5)$$

$$(\ln \eta_r)/c = [\eta] + (k' - 1/2)[\eta]^2 c \quad (6)$$

$\eta_r$  is the flow time ratio between the solution and the solvent,  $\eta_{sp} = \eta_r - 1$ , and  $k'$  is an empirical constant. Extrapolation of  $(\ln \eta_r)/c$  and  $\eta_{sp}/c$  to infinite dilution should result in the same intercept, which is  $[\eta]$ .

## Results and Discussion

**Polymer Synthesis.** Polymerization of AHBAH at concentrations below 14.5 wt % resulted in solutions that remained optically isotropic in contrast to those of slightly higher concentration that became optically anisotropic at early stages. The effect on the intrinsic viscosity of the resulting polymer by reacting in the nematic phase was pronounced. Comparing ABPBO-2f with ABPBO-5 (see Table II) shows that polymerizing in the isotropic phase results in a substantially lower degree of polymerization (700 versus 350). When ABPBO was polymerized at a polymer concentration of 13.6 wt %, which is below the critical concentration for formation of the nematic phase (even at a degree of polymerization of 350), the intrinsic viscosity was limited to 9.2 dL/g. On the other hand, an intrinsic viscosity of 18.0 dL/g was obtained when ABPBO was polymerized at 2.9 wt % higher, a concentration at which the nematic phase forms when the polymer reaches an average degree of polymerization of approximately 40. The onset of the nematic phase was determined by the appearance of stir-opalescence in the reaction mixture.

The effect of polymerization temperature can be seen in Figure 2, in which the apparent degree of polymerization as a function of time is plotted for three polymerizations conducted at 200, 185, and 175 °C. Samples of the polymerization mixture were removed at various times, and the intrinsic viscosities were measured. In the polymerization conducted at 200 °C, the apparent decrease in the degree of polymerization with time may be explained by

**Table III**  
Experimental Results and Theoretical Calculations of the Effects of End Capping on Molecular Weight

	experimental			theoretical $x_n$		
	% end cap	$M_w$	$x_n$	$p = 1.00$	$p = 0.998$	$p = 0.990$
<b>ABPBT</b>						
-1	0.0	111 000	415.4	$\infty$	500.0	100
-2	0.0	50 000	188.0	$\infty$	500.0	100
-4	0.5	33 100	123.1	201	143.6	67.0
-5	1.0	13 700	51.7	101	84.2	50.5
-6	5.0	5 300	20.1	21	20.2	17.5
-7	10.0	3 600	13.4	11	10.8	10.0
<b>ABPBO</b>						
-1	0.0	113 000	474.4	$\infty$	500.0	100
-7	0.5	32 000	133.6	201	143.6	67.0
-8	1.0	26 000	108.4	101	84.2	50.5
-9	5.0	4 900	20.5	21	20.2	17.5

samples having extensive crystallization that does not fully dissolve during the viscosity measurement. This aggregation phenomenon was observed by Berry<sup>10,11</sup> for the more rigid benzazole polymer PBO and heterocyclic polymer BBL. We saw no evidence of aggregation in the samples analyzed by light-scattering techniques, which were all polymerized at 185 °C. Even though the polymerization rate is significantly enhanced by heating at 200 °C, such an aggregation or crystallization would be expected to be detrimental to subsequent processing, and the optimal temperature for polymerization was therefore chosen to be 185 °C.

In contrast with a typical polymerization of PBT at 185 °C, the polymerization of AHBAH occurs over a much longer period (see Figure 2). This observation could be explained by a greater decrease in reactivity with increasing molecular weight because of the difference in molecular rigidity or by a lower stability of the PBT monomer compared to the carboxyl-stabilized AB monomer. The apparent extent of reaction of the end-capped ABPBZ systems, as discussed below, also appears to be greater than for PBT.

The effect of PPA composition at the end of the polymerization, or final  $P_2O_5$  content ( $P_3$ ), on the attainable molecular weight can be seen by comparing those polymerizations having  $P_3$  of 82.2% with those having  $P_3$  of 83% or higher. Polymerizations with higher  $P_2O_5$  contents in general have considerably higher molecular weights. We believe this effect is due to the need to maintain an effective concentration of species that perform functions such as hydrolysis of the water of condensation and activation of the functional groups. An upper limit of about 84% final  $P_2O_5$  content was imposed to control solution viscosity and allow for efficient mixing of reactants.

**Effect of End Capping on Molecular Weight.** Flory's theory<sup>12</sup> for the depression of molecular weight by nonequivalence of functional groups and the presence of monofunctional reagents can be used to analyze the results of polycondensation reactions of ABPBT and ABPBO with end-capping agents. The number-average degree of polycondensation,  $x_n$ , is given by

$$x_n = (1 + r) / \{2r(1 - p) + 1 - r\} \quad (7)$$

where  $p$  is the extent of reaction ( $p$  = moles of monomer condensed/total moles of monomer), and  $r$  = moles of monomer/(moles of monomer + 2 × moles of end capper). Degree of polymerization can then be calculated for known values of  $p$  using eq 7.

Assuming a polydispersity ( $M_w/M_n$ ) of 2 for these ABPBZ polymers, we can calculate the experimental values of  $x_n$  from  $M_w$  as tabulated in Table III. The data are also

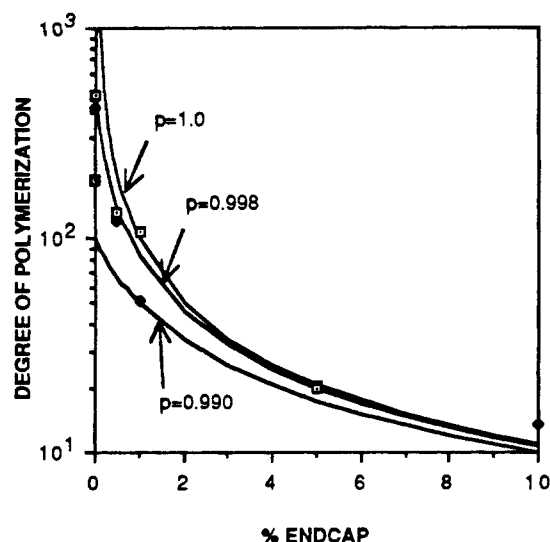


Figure 3. Effects of end capping on the degree of polymerization of ABPBT (◆) and ABPBO (◻). Solid lines represent predictions of Flory's theory at various extents of reaction,  $p$ .

Table IV  
Polymerizations of AHBAH in MSA/ $P_2O_5$  Mixtures

ABPBO	C, %	Y, %	MSA/ $P_2O_5$ , <sup>a</sup> g	$P_2O_5$ , g	total $P_2O_5$ , %	PT, <sup>b</sup> h	$[\eta]$ , dL/g
-10	17.5	15.0	38.36	27.65	44.6	49	16.0
-11	17.6	15.0	44.60	20.89	35.7	46	4.75
-12	19.0	18.0	47.36	16.60	30.2	24	<1

<sup>a</sup> 10 wt %  $P_2O_5$  dissolved in MSA by stirring for 2 h. <sup>b</sup> Length of time that the monomer/MSA/ $P_2O_5$  mixture was heated at 150 °C.

plotted in Figure 3. The solid lines in Figure 3 are the theory predictions of  $x_n$  as a function of percent end capping when  $p = 1.0, 0.998$ , and  $0.990$ . Comparison between the theoretical and experimental values of  $x_n$  demonstrates that the effect of end capping can be modeled by Flory's theory for condensation polymerization in spite of the stiff polymer backbone structure by assuming various extents of reaction.

**Polymerization in Mixtures of Methanesulfonic Acid and  $P_2O_5$ .** Three polymerizations of AHBAH were conducted by adding various amounts of  $P_2O_5$  to methanesulfonic acid (MSA) that contained 10 wt %  $P_2O_5$ . MSA containing 10 wt %  $P_2O_5$  has been described as a convenient alternative to PPA.<sup>13</sup> However, we found that greater than 40 wt %  $P_2O_5$  was required during the polycondensation if concentrations in the 17–19 wt % region were employed. MSA was heated with 10 wt %  $P_2O_5$  for 2 h according to the published procedure. This homogeneous solvent was then used for the dehydrochlorination. The additional  $P_2O_5$  was added in a manner analogous to the  $P_2O_5$  adjustment of PPA. The results of these polymerizations are summarized in Table IV. Polymerization temperature was limited to 150 °C because of decomposition of the solvent at higher temperatures. Attempts to polymerize the more oxidatively sensitive mercapto analogue MABAH gave black, nonpolymeric products, presumably owing to extensive side reactions.

**Solution Characterization.** The LALS and viscometry data are tabulated in Tables V and VI for ABPBT and ABPBO, respectively. The Mark-Houwink-Sakurada (MHS) constants,  $K$  and  $a$ , of the empirical relation

$$[\eta] = KM_w^a \quad (8)$$

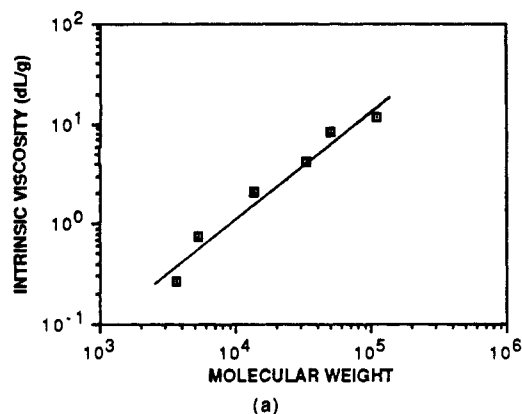
can be determined by a double-logarithmic plot of  $[\eta]$  as a function of weight-average molecular weight ( $M_w$ ) as shown in Figure 4. A least-squares analysis of the ex-

Table V  
Light-Scattering and Intrinsic Viscosity Measurements for ABPBT Solutions

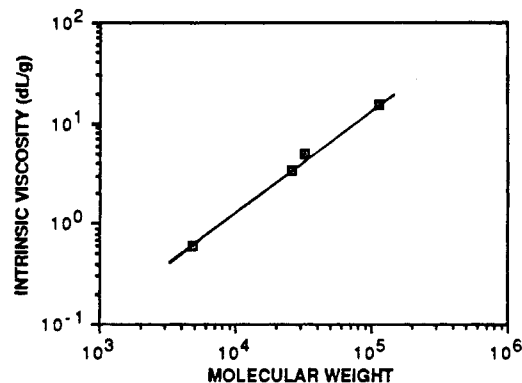
ABPBT	EC %	$M_w$	$\delta^2$	$A_2$	$[\eta]$ , dL/g
-1	0.0	111 000	0.028	0.0101	11.5
-2	0.0	50 000	0.083	0.231	8.14
-4	0.5	33 000	0.058	0.0099	4.18
-5	1.0	13 700	0.095	0.0107	2.11
-6	5.0	5 300	0.117	0.0212	0.758
-7	10.0	3 600	0.124	0.0251	0.272

Table VI  
Light-Scattering and Intrinsic Viscosity Measurements for ABPBO Solutions

ABPBO	EC %	$M_w$	$\delta^2$	$A_2$	$[\eta]$ , dL/g
-1	0.0	113 000	0.032	0.0078	15.0
-7	0.5	32 000	0.052	0.0094	4.95
-8	1.0	26 000	0.067	0.0125	3.39
-9	5.0	4 900	0.092	0.0247	0.618



(a)



(b)

Figure 4. Double-logarithmic plots of intrinsic viscosity and molecular weight to determine the Mark-Houwink-Sakurada constants for (a) ABPBT and (b) ABPBO.

perimental results indicates that the MHS relation may be written as

$$[\eta] = 1.26 \times 10^{-4} M_w^{1.00} \quad \text{for ABPBT} \quad (9)$$

$$[\eta] = 1.09 \times 10^{-4} M_w^{1.02} \quad \text{for ABPBO} \quad (10)$$

within the molecular weight range 2000–200 000.

The MHS exponents are found to be about unity experimentally for both polymers. Their values are between 1.8 for rodlike polymers (such as PBT) and 0.5 for random coil polymers (such as polyethylene) in  $\theta$  solvent, indicating that this class of poly(benzazoles) is characterized by an intrinsically semirigid structure.

The second virial coefficient,  $A_2$ , was found to be about 0.01–0.02 cm<sup>3</sup> mol/g<sup>2</sup> for both ABPBT polymers. Compared with many hydrocarbon polymers in organic sol-

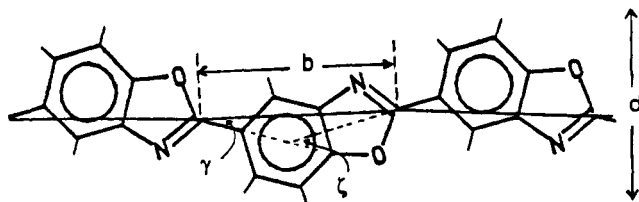


Figure 5. Schematic diagram illustrating the determination of molecular parameters needed for the wormlike model calculations.

vents,<sup>14</sup>  $A_2$  for these protonated, heterocyclic aromatic polymers is 1–2 orders of magnitude higher, indicating strong polymer/solvent interactions.

We found no evidence of the formation of intermolecular aggregation in these solutions under our experimental conditions, although such an effect appears to be commonly observed in other protonated chains in strong acids.<sup>10,11</sup>

**Model Comparison with Solution Properties.** A wormlike cylinder model has been proposed by Yamakawa and Fujii<sup>15</sup> to evaluate the intrinsic viscosity of stiff chains. The model requires three molecular parameters—contour length  $L$ , persistence length  $\rho$ , and molecular diameter  $d$ —to evaluate the intrinsic viscosity  $[\eta]$ :

$$[\eta] = \Phi(L/\rho)^{3/2}\rho^3/M \quad (11)$$

$\Phi$  is a function of  $L/\rho$  and  $d/\rho$ , and  $M$  is the molecular weight.

A comparison of the experimental results to the Yamakawa–Fujii model can be made using an iterative scheme assuming values of  $\rho$  and  $d$  until the agreement of the theoretical calculations to the data is acceptable. Alternatively, we estimated  $\rho$  and  $d$  for these ABPBZ polymers using the independent theoretical guidance described below.

Flory and co-workers have proposed a virtual bond model<sup>16</sup> to evaluate persistence vectors of polymers having catenation angles less than  $180^\circ$ . If  $\gamma$  is the acute angle between consecutive ring axes,  $\zeta$  is the angle between the virtual bond and the exocyclic bond, the  $b$  is the virtual bond length as shown in Figure 5, then  $\rho$  can be estimated as

$$\rho = b[(u + \beta v)/(1 - \alpha)] \quad (12)$$

where  $\alpha = \cos \gamma$ ,  $\beta = \sin \gamma$ ,  $u = \cos \zeta$ , and  $v = \sin \zeta$ . The values of persistence length estimated by this model should be regarded as upper bound values and have compared favorably with the experimental results on *p*-phenylene polyamides and polyesters.<sup>16</sup>

We estimated  $\rho$  for ABPBT and ABPBO based on their molecular geometry such as bond lengths and bond angles taken from X-ray crystallographic results on oriented fibers.<sup>17</sup> For ABPBT,  $\gamma = 18^\circ$ ,  $\zeta = 16.2^\circ$ ,  $b = 6.08$  Å, and  $\rho = 130$  Å. For ABPBO,  $\gamma = 30^\circ$ ,  $\zeta = 17^\circ$ ,  $b = 5.90$  Å, and  $\rho = 50$  Å. ABPBO has a lower value of  $\rho$  because of its higher value of  $\gamma$ .

In addition to  $\rho$ ,  $d$  is required to calculate  $[\eta]$  from the Yamakawa and Fujii model. We estimated  $d$  for the ABPBZ polymers using the orthogonal distance from the extended chain axis to the atom farthest from the axis as illustrated in Figure 5. This estimate yields  $d = 5.5$  Å for ABPBT and  $7.5$  Å for ABPBO. Table VII summarizes the theoretical estimates of  $\rho$  and  $d$ . These values can then be used to calculate  $[\eta]$  as a function of  $M$  according to eq 11 and the numerical values of  $\Phi$  given in ref 15. The contour length  $L$  is determined from  $L = M/M_L$ , where  $M_L$  is a shift factor equal to 21.88 daltons/Å (133 daltons/6.08 Å) for ABPBT and 19.83 daltons/Å (117 daltons/5.90 Å) for ABPBO.

Table VII  
Molecular Parameters for ABPBT and ABPBO Molecules

parameter	ABPBT	ABPBO
$\zeta$	$18^\circ$	$30^\circ$
$\gamma$	$16.2^\circ$	$17.0^\circ$
$b$	6.08 Å	5.90 Å
$\rho$	130 Å	50 Å
$d$	5.5 Å	7.5 Å

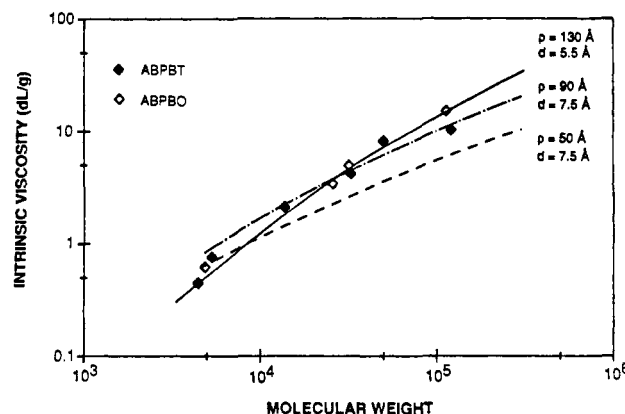


Figure 6. Comparison of experimental results and model predictions of the Mark-Houwink-Sakurada relationships for ABPBO and ABPBT.

Both the experimental results and theoretical model calculations of  $[\eta]$  versus  $M_w$  for ABPBT and ABPBO are plotted in Figure 6. The solid line is the wormlike cylinder model prediction using  $d = 5.5$  Å and  $\rho = 130$  Å for ABPBT. Model comparison with the ABPBT experimental data (open diamonds) is very good. The broken line represents the model calculation obtained for ABPBO based on the value of  $d = 7.5$  Å and  $\rho = 50$  Å. In this case, the model fits poorly with the ABPBO results (filled diamonds). This discrepancy can be greatly reduced by increasing  $\rho$  from 50 to 90 Å for ABPBO as indicated by the dash-dot line.

A number of factors may account for the discrepancy in the value of persistence length estimated by Flory's virtual bond treatment and that determined by fitting the Yamakawa–Fujii model to our experimental results. ABPBZ chains, when dissolved in strong protic acid such as MSA, are protonated and therefore should be described as macroions. Electrostatic interactions among chain elements can affect the dilute solution conformation of the polyelectrolyte molecule to assume a more extended one in equilibrium, thereby increasing the persistence length of the chain.<sup>18–20</sup> In such a case,  $\rho$  may be written as

$$\rho = \rho_e + \rho_c \quad (13)$$

where  $\rho_e$  is the electrostatic contribution and  $\rho_c$  is the conformational and steric contribution to the persistence length.

Polydispersity in the molecular weight of our polymer samples may also be a factor in the quantitative difference between theory and experiments. Finally, the excluded volume effect, not accounted for in the Yamakawa–Fujii model, may be another reason for the disagreement.

In Figure 6, the theory predictions show a gradual increase in slope (hence an increase in the value of the HMS exponent) with decreasing  $M_w$  for semirigid chains. In contrast, flexible chains have been reported to exhibit a constant HMS exponent over many decades of  $M_w$ .<sup>21</sup> Because the accuracy of our experimental results does not permit clear differentiation of such a slight change in slope, more accurate viscometry and molecular weight measurements over a wider range of molecular weights are

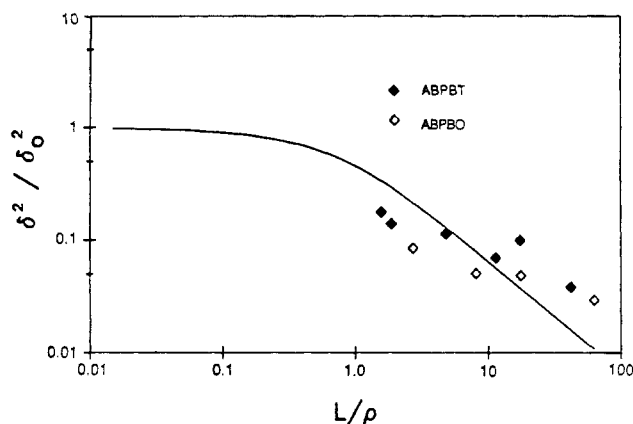


**Figure 7.** Comparison of experimental results and model predictions of normalized anisotropy factor ( $\delta^2/\delta_0^2$ ) as a function of normalized length ( $L/\rho$ ).

needed to confirm this prediction by the wormlike chain model.

Figure 7 plots the LALS results of  $\delta^2/\delta_0^2$  versus  $L/\rho$ . The solid line represents the model calculations using eq 2. The anisotropy factor  $\delta^2$  has been normalized by the intrinsic anisotropy  $\delta_0^2$ , which was estimated after model comparisons with experimental data were made. Experimentally determined  $\delta_0^2$  is 0.84 for ABPBT and 1.10 for ABPBO. The measured molecular weight was first reduced to the contour length  $L$  then normalized by the persistence lengths with  $\rho = 130$  Å for ABPBT and  $\rho = 90$  Å for ABPBO. Comparison of the experimental data with the model prediction is satisfactory. The scatter in the data points is most likely due to the difficulty in obtaining good measurements of  $R_{H_V}$ .

### Concluding Remarks

Our study indicates that ABPBT and ABPBO are characterized by persistence lengths of 90–130 Å, which are in fair agreement with the virtual bond model predictions. This comparison suggests that these extended-chain polymers assume a near random distribution of cis and trans conformations, with a slight preference for the trans conformation due to intramolecular electrostatic interactions, in dilute solution. At concentrations above ~14 wt %, ordered phases form during polymerization, and the trans conformation is believed to dominate to allow this phase change.

**Acknowledgment.** This work was supported by the Air Force Office of Scientific Research under Contract F49620-85-K-0015. We also thank Professor Guy Berry for some useful discussions on polyelectrolyte molecules.

**Registry No.** AHBAH, 1571-65-9; AHBAH (homopolymer), 29692-05-5; MABAH, 1571-66-0; MABAH (homopolymer), 29895-61-2; PABA, 150-13-0; ACBTH, 93-85-6; ABPBO (SRU), 89718-41-2; ABPBT (SRU), 32105-21-8; NaSCN, 540-72-7;  $P_2O_5$ , 1314-56-3; *p*-hydroxybenzoic acid, 99-96-7; benzoic acid, 65-85-0; nicotinic acid, 59-67-6.

### References and Notes

- (1) Wolfe, J. F.; Loo, B. H.; Arnold, F. E. *Macromolecules* **1981**, *14*, 915.
- (2) Wolfe, J. F.; Arnold, F. E. *Macromolecules* **1981**, *14*, 909.
- (3) Chow, A. W.; Hamlin, R. D.; Sandell, J. F.; Wolfe, J. F. *Mesophase-Enhanced Polymerization and Chemo-Rheology of Poly(p-phenylenebenzobisthiazole)*. *Materials Research Society Symposium Proceedings*; Adams, W. W., Eby, R. K., McLemore, D., Eds.; Materials Research Society: Pittsburgh, 1988; Vol. 134, in press.
- (4) Wolfe, J. F.; Sybert, P. D.; Sybert, J. R. US Patent 4,533,693, Aug 1985 (to SRI International).
- (5) Hwang, W.-F.; Wiff, D. R.; Benner, C. L.; Helminiak, T. E. *J. Macromol. Sci., Phys.* **1983**, *B22*, 231.
- (6) Jannelli, L.; Giordano-Orsini, P. *Gazz. Chim. It.* **1958**, *88*, 331.
- (7) Wolfe, J. F. In *Encyclopedia of Polymer Science and Engineering*, 2nd ed.; Mark, H. F., et al., Eds.; Wiley: New York, 1988; Vol. 11, p 601.
- (8) Horn, P. *Ann. Phys.* **1966**, *10*, 386.
- (9) Nagai, K. *Polym. J.* **1972**, *3*, 67.
- (10) Berry, G. C. *J. Polym. Sci.; Polym. Symp.* **1978**, *65*, 143.
- (11) Wong, C.-P.; Ohnuma, H.; Berry, G. C. *J. Polym. Sci.; Polym. Symp.* **1978**, *65*, 173.
- (12) Eaton, P. E.; Carlson, G. R.; Lee, J. T. *J. Org. Chem.* **1973**, *38*, 4071.
- (13) Flory, P. J. *Principles of Polymer Chemistry*; Cornell University Press: Ithaca, NY, 1953; pp 92–93.
- (14) Brandrup, J.; Immergut, E. H., Eds., *Polymer Handbook*, 2nd ed.; Wiley: New York, 1975; p IV-91.
- (15) Yamakawa, H.; Fujii, M. *Macromolecules* **1974**, *7*, 128.
- (16) Erman, B.; Flory, P. J.; Hummel, J. P. *Macromolecules* **1980**, *13*, 484.
- (17) Fratini, A. V.; Cross, E. M.; O'Brien, J. F.; Adams, W. W. *J. Macromol. Sci., Phys.* **1985–86**, *B24*, 159.
- (18) Berry, G. C. *Properties of Solutions of Rodlike Chains from Dilute Solutions to the Nematic State*. *Materials Research Society Symposium Proceedings*; Adams, W. W., Eby, R. K., McLemore, D., Eds.; Materials Research Society: Pittsburgh, 1988; Vol. 134, in press.
- (19) Fixman, M. *J. Chem. Phys.* **1982**, *76*, 6364.
- (20) Davis, R. M.; Russel, W. B. *J. Polym. Sci., Polym. Phys.* **1986**, *24*, 511.
- (21) Fujita, H. *Macromolecules* **1988**, *21*, 179.